ELSEVIER

Journal of Nuclear Materials 256 (1998) 145–154

journal of nuclear materials

High-temperature Knudsen cell studies of cesium iodide in hyperstoichiometric uranium dioxide

J. McFarlane *, J.C. LeBlanc

Containment Analysis Branch, Reactor Safety Division, AECL-Whiteshell Laboratories, Pinawa, Man., Canada R0E 1L0

Received 4 November 1997; accepted 8 April 1998

Abstract

The stability of cesium iodide in the presence of UO_{2+x} was investigated at temperatures up to 2300 K and for $0.00 < x < 0.29$ in a Knudsen-cell mass-spectrometric apparatus. Heating of CsI and hyperstoichiometric urania, $UO_{2.29}$, to 900 K produced $Cs_2U_4O_{12}$ with a reaction yield of about 50%. Most of the unreated CsI starting material was volatilized below 1000 K. The decomposition of $Cs_2U_4O_{12}$ was observed between 1250 and 1800 K, producing atomic cesium observable in the mass spectrometer. At these temperatures, the oxygen potential of the chemical system appeared to be controlled by the UO_{2+x}. © 1998 Published by Elsevier Science B.V. All rights reserved.

PACS: 82.60.H; 28.41.T; 82.60.cx; 82.80.K

1. Introduction

In the event of a severe nuclear accident, radioiodine is a fission product that can have a deleterious effect if it is released from the reactor containment building. Because of the excess of cesium to iodine in fission yield (10 to 1), it is thought that over 99.9% of iodine will exist in the form of CsI under most accident conditions [1]. Because CsI has a high melting point, 903.5 K [2], it is involatile outside the core and will likely be dissolved in the cooling water collected in the containment sump.

Under oxidizing conditions, however, other compounds of cesium can become more thermodynamically stable than CsI, e.g., Cs_2MoO_4. The formation of cesium molybdate under normal reactor operating conditions has been suggested by Matzke [3], after extremely long irradiation times (i.e., corresponding to localized burn-ups in excess of 1900 MW h/kg U), which can lead to a significant amount of excess oxygen in the urania lattice. As hypothesized for some accident scenarios, fuel oxidation by the interaction of UO_2 with steam, Eq. (1) can be a very important phenomenon.

$$UO_2 + xH_2O \Rightarrow UO_{2+x} + xH_2 \text{ (above 1320 K in steam).} \quad (1)$$

Under these conditions, much of the fission-product inventory may be released because of changes in the microstructure of the fuel and also because of the formation of volatile oxides i.e., [4]. Mitigation of the consequences of a severe accident is a key consideration in the design of a nuclear power reactor. Computer modelling of accident scenarios is a tool for understanding the sequence of events and physical phenomena that govern fission-product and fuel behaviour. Because it is difficult to reproduce such complex events in a laboratory, or in a research reactor, much of the code validation is based on small-scale studies, each of which focusses on a single parameter. In this case, conditions of the actual experiment are not set up to emulate an accident scenario, but are designed to explore the full range of a single parameter such as temperature, holding other parameters, such as chemical composition, constant.

In this study the stability of CsI in the presence of UO_{2+x} was investigated, with x varying from 0.00 to 0.29. Vapour pressures were recorded using a Knudsen-cell mass-spectrometric apparatus. The volatile species were identified using appearance potential and

---

[*] Corresponding author.

0022-3115/98/$19.00 © 1998 Published by Elsevier Science B.V. All rights reserved.
PII: S 0 0 2 2 - 3 1 1 5 (9 8) 0 0 0 6 4 - 6

fragmentation data. The condensed-phase residue was analyzed by X-ray powder diffractometry. From these data, the reactive behaviour of the cesium–iodine–UO_{2+x} system was investigated up to 2000 K.

2. Experimental

2.1. Apparatus

The Knudsen-cell apparatus consisted of two stainless steel evacuated chambers, separated by a 3.18-mm hole (top aperture), Fig. 1, and a shutter that could be manipulated from outside the vacuum envelope. One chamber contained an inductively heated Knudsen cell, and the other a Finnigan quadrupole mass spectrometer separated by a water-cooled aperture (hole diameter of 3.2 mm). Both could be evacuated to a minimum pressure of 10^{-5} Pa, by a Seiko–Seiki turbomolecular pump and a diffusion pump, respectively. The former was also able to handle outgassing from the cell or the sample or from both, and maintained the Knudsen-cell chamber vacuum below 7×10^{-4} Pa.

The Knudsen cell had an ID of 12.7 mm, a length of 34.0 mm, and an orifice size of 0.7 mm, giving a Clausing factor of 0.21 [5] and a ratio of orifice size to sample area of 0.01. Volatile species effusing from the cell orifice were ionized by electron bombardment at 70 eV, 0.50 mA emission, to produce positive ions, and these were detected with a Finnigan quadrupole mass analyzer. For appearance-potential measurements, the emission was reduced to 0.05 mA to stabilize the signal at low electron energies. Before and after an experiment, the sensitivity of the mass spectrometer was checked using a calibrated leak of perfluorotributylamine (FC43), which was occasionally compared to a silver reference. Mass spectra were collected on a Gateway 2000 P4D-66, 486 computer using Shrader data acquisition software. Analysis was performed using a Labview program and a Quattro–Pro spreadsheet.

In the series of experiments looking at the reaction of CsI with UO_{2+x}, it was discovered that compounds containing cesium were particularly difficult to contain [6]. Tantalum was selected as the cell material, since it is corrosion resistant and has a high melting point (3273 K). In addition, a 1-to-2-μm layer of iridium was deposited

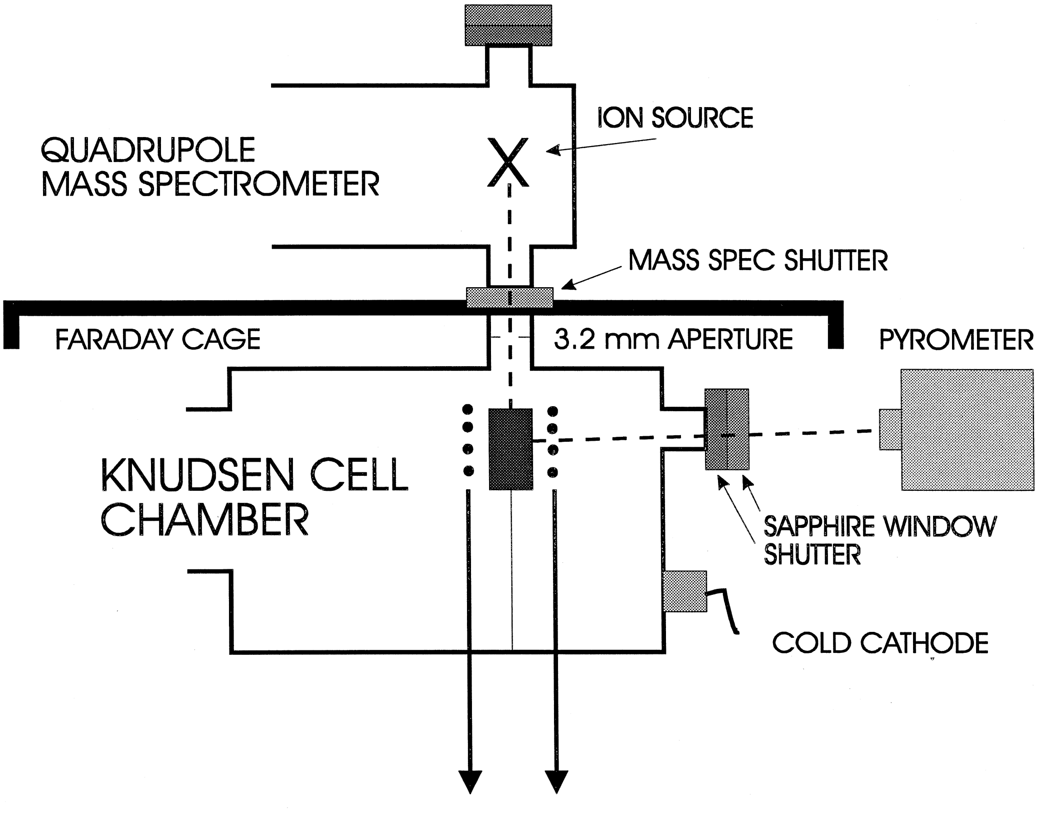

Fig. 1. Schematic of Knudsen-cell mass-spectrometric apparatus.

on the inside surfaces of both the body and the lid of newly machined tantalum cells (sputtering done by Alberta Microelectronic Centre, Edmonton, Canada). Iridium is quite soluble in tantalum above 1873 K (up to 7.7 wt%), but there was no evidence to suggest that diffusion of the iridium coating into the tantalum, or formation of intermetallic compounds (possible above 2226 K) [7] affected the chemistry of the CsI – UO_{2+x} system.

The cesium iodide used was 99.999% pure from Aesar. The UO_2 was obtained from CANDU®(CANDU® is a registered trademark of Atomic Energy of Canada Limited) fuel pellets (0.7 wt% ^{235}U), which were crushed and sieved to obtain particle sizes between 20 and 160 μm. The stoichiometry of unirradiated CANDU fuel is specified as $UO_{2.0003\pm0.0002}$ [8], and the sample used in these tests was analyzed gravimetrically to be $UO_{2.00\pm0.01}$. Some of the unirradiated fuel was pre-annealed in a sealed vial at 673 K for 3 d. Although some air was present in the vial before sealing, there was no significant change in the stoichiometry of the urania, as measured by gravimetry. Samples were prepared for the cell by weighing out 3 g of UO_2 and about 0.12 g of CsI powder to obtain about 4% CsI by weight in $UO_{2.00}$. The two compounds were mixed with a spatula and were added to the cell. The UO_2 stock was kept in an argon-filled desiccator to prevent further oxidation. The CsI stock was kept dry in a desiccator.

In some of the tests, highly oxidized urania was used, consisting of mixed phases but mainly U_4O_9, and analyzed gravimetrically to be $UO_{2.29\pm0.01}$. Analysis of this material by scanning electron microscopy (SEM) showed that it was composed of individual particles, 10 μm diameter, and soft (easily crushed with a spatula) 40 μm diameter clumps made up of the smaller particles. The hyperstoichiometric urania was heated with 5 and 11.4 wt% CsI in separate tests.

Some of the appearance potential measurements were performed using a mixture of CsI + $UO_{2.11}$, the latter having been prepared by oxidation of UO_2 on exposure to the ambient air of the laboratory.

2.2. Method

Two types of experiments were performed in the Knudsen cell. One involved the acquisition of ion intensities as a function of temperature in both the ascending and the descending temperature-ramp mode, the latter being a preferable approach [9]. The other involved the measurement of ion signal at a fixed temperature as a function of ascending electron-energy ramp, to give an appearance potential for the ion. Data were collected by selecting the temperature or electron energy of interest and waiting 30 s after the shutter to the mass spectrometer was opened before collecting a mass spectrum. In addition, two background scans were collected (shutter closed), one before and another after each scan. This methodology was established to minimize contributions from a time-dependent signal that arose from movement of the shutter.

Post-test X-ray diffraction (XRD) analysis of the residues from heating was also used to help identify the condensed phases present at a particular temperatures. Power to the induction coils was switched off, and the sample was cooled several hundred degrees within a few minutes. Only small samples, 50 μg, were removed so that enough of the residue remained in the cell to continue the heating experiment. The sensitivity of the XRD analysis was about 4 wt% for these samples.

2.3. Calibration procedures

2.3.1. Temperature measurements

The temperature of the cell body was obtained by focussing a pyrometer into a black-body cavity on the side of the cell. Four pyrometers were used, which covered the temperature range from 625 to 3000 K (the maximum temperature to which the cell was heated). The lower-temperature pyrometer was a single-wavelength instrument, whereas the other three were dual wavelength. Calibration of the temperature measurements was done in situ, previously described in detail [10], using the melting points of aluminum (933 K), gold (1337 K) and platinum (2041 K). The precision of the measurements was ±0.4% for the single wavelength pyrometer (650 to 1000 K) and ±0.2% for the dual wavelength pyrometers (up to 2600 K). The accuracy of the temperature readings was estimated to be within ±0.8% up to 2300 K.

2.3.2. Vapour pressure measurements

The vapour pressure, p, of the effusing gas was calculated from the ion intensity, I, at temperature, T, using the expression

$$p = \frac{IT}{\sigma\gamma\eta f s k_{\mathrm{Ag}}}. \qquad (2)$$

Parameters related to the precursor are the ionization cross-section, σ [11], and the isotopic abundance, η. The expression also includes a correction for the sensitivity of the instrument as determined from the FC43 calibrated leak, s, and a correction for the area of the orifice, f. The mass dependence of the quadrupole analyzer and electron multiplier, γ, was determined by analysis of the fragmentation pattern of FC43. Other effects, such as that of geometry, are included in the k_{Ag} term, which was derived from a calibration with silver. Vapour pressure measurements were determined from data gathered during a decending temperature ramp. The accuracy of these measurements depended greatly on the chemical system being studied, but most uncertainty arose from the values used for the ionization cross sections at

70 eV, which were not directly available for the molecular species. It was estimated that vapour pressure could be measured to within a factor of 2.

2.3.3. Appearance potential measurements

Appearance potentials were determined from the plots of ion intensity versus electron energy, as the intersection of the linear portion of the plot with the abscissa. The filament voltage was calibrated with appearance potentials measured for the permanent gases, N_2, O_2, H_2O and CO_2, and for silver and argon introduced into the cell. Uncertainties on the measured appearance potentials were determined to be ±0.2 eV below 10 eV, and ±2% above 10 eV.

3. Results and discussion

The results of the Knudsen cell experiments are summarized in Tables 1–3. In Table 1 are presented the ions observed in the Knudsen cell as the samples were heated from 600 to above 2000 K. Second law heats of vaporization were calculated from the slopes of the Clausius–Clapeyron plots and are presented in Table 2, along with the corresponding vaporization or reaction process. In Table 3 are shown the measured appearance potentials for the cesium ions observed at different temperatures.

3.1. CsI

A control experiment was performed by heating pure CsI in a tantalum cell, to provide a baseline against which the reactive $CsI - UO_{2+x}$ systems could be compared. The data for Cs^+ are shown on a Clausius–Clapeyron plot, Fig. 2. The sensitivity of the experiment is approximately 10^{-2} Pa. The solid line shows published data on the vapour pressure of CsI [2]. Because the cesium ion was the major ion observed above CsI, the data points need only be multiplied by a factor of 1.2 for a direct comparison with the solid line, an amount too small to show up on this logarithmic plot. This factor accounts for the minor ions, CsI^+, I^+, as well as the small amounts of Cs_2I^+, Cs^{++} and I^{++}. About 1% of the cesium iodide was volatilized in the dimeric form, $(CsI)_2$, parent of Cs_2I^+ ($m/z = 393$). There is reasonable agreement between the absolute vapour pressure of CsI measured in this experiment and the literature values, within a factor of 2.

The heat of vaporization of CsI(c) to CsI(g), $\Delta_v H^0_{298\ K}$, calculated using the third-law method [12], was 198 ± 3 kJ mol^{-1}, and is close to that reported by Cordfunke and Konings [2] or 193 ± 2 kJ mol^{-1}. Above 1000 K, the signal levels dropped below the detection limit of the apparatus, 10^{-2} Pa, indicating that the CsI was depleted from the Knudsen cell. At very high temperatures, above 1700 K, the cesium ion signal is again above background.

There are a number of explanations for the small amount of cesium seen at very high temperatures. Similar high-temperature cesium signal was observed for the $CsI + UO_{2+x}$ mixtures, and in an earlier study of the heating of pure $Cs_2U_2O_7$ [13]. In all of these cases elemental cesium could have deposited on surfaces in the vacuum chamber, to be revolatilized as the Knudsen cell was heated past 2000 K. The high temperature cesium seen above the mixtures of CsI and UO_{2+x} may have had contributions from the decomposition of ternary phases, such as $Cs_2U_6O_{18}$, or from volatilization of cesium dissolved in UO_2 (solubility of 0.16 ± 0.04 wt% cesi-

Table 1
Knudsen cell results

Temperature range (K)	Ions and intensities relative to major ion	Precursor in gas phase
600–1000	I^+(1.0), I_2^+(0.6)	I_2
700–1000	Cs^+(1.0), I^+(0.25), CsI^+(0.1), I^{++}(0.02), Cs^{++}(0.01)	CsI
	Cs_2I^+ (0.005)	Cs_2I_2
1000–1250	Cs^+(1.0), I^+(0.23), CsI^+(0.01), Cs^{++}(0.03)	CsI
1250–1800	Cs^+(1.0), Cs^{++}(0.17)	Cs
1800–2000	Cs^+(1.0)	Cs
2000+	UO_2^+(1.0), UO^+(0.6), UO_2^{++}(0.4), UO^{++}(0.26)	UO_2

Table 2
Postulated reactions of $CsI + UO_{2+x}$

Temperature range (K)	$\Delta_v H$ (kJ mol^{-1}) Second law	Reaction
600–800	Not measurable	$2CsI(s) + (\frac{4}{x})UO_{2+x}(s) \Rightarrow Cs_2U_4O_{12}(s) + I_2(g) + (\frac{4}{x})(1-x)UO_2(s)$
800–1000	160 ± 20	$CsI(c) \Rightarrow CsI(g)$
980–1250	280 ± 80	$CsI(ad) \Rightarrow CsI(g)$
1250–1800	340 ± 60	$Cs_2U_4O_{12}(s) \Rightarrow 2Cs(g) + 4UO_2(s) + 2O_2(g)$

Table 3
Appearance potentials of cesium ions observed above CsI – UO_{2+x}

Appearance potential of Cs^+ (±0.2 eV)	Temperature (K)	Precursor	Literature appearance potential values [15]
7.8	746	CsI	7.3–8.3
7.5	893	CsI	
7.6	1146	CsI	
7.2	1248	CsI	
3.8	1629	Cs	3.984

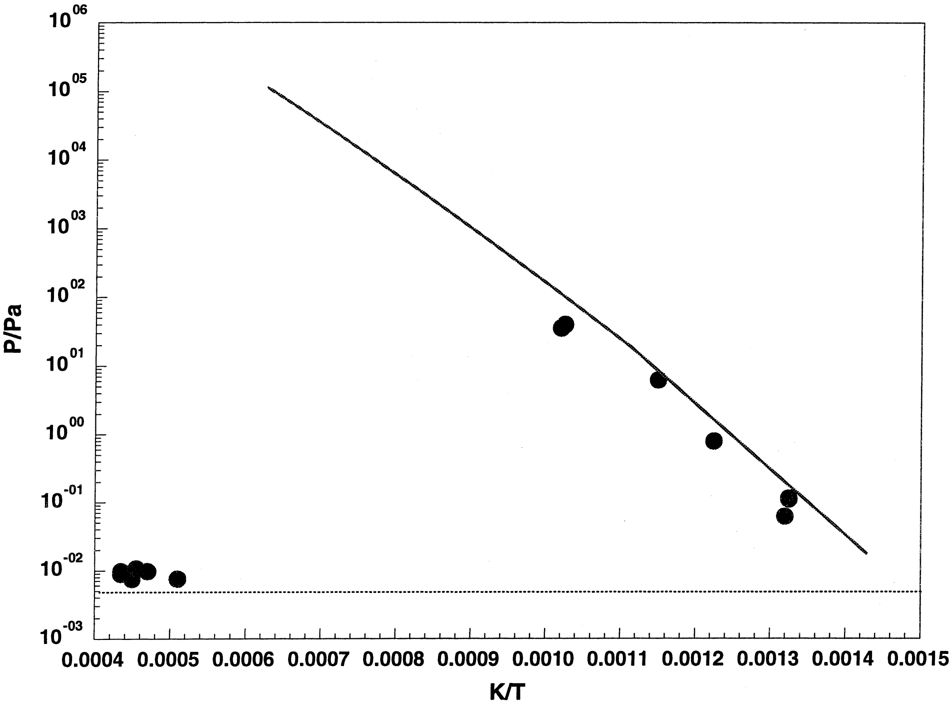

Fig. 2. Partial pressure (Pa) of cesium compounds as a function of reciprocal temperature (K^{-1}). Circles represent data collected in the current experiment. The solid line is published vapour-pressure data for CsI [2]. The dashed line indicates the detection limit of the experiment.

um at 2173 K [14]). Neither of these explanations describe the data very well, in the first case because the signal for the mixture of $UO_{2.00}$ was about the same as the signal for the mixture of $UO_{2.29}$, which produced much more uranate. And the temperature profile of the Cs^+ was quite different from that of the ions from the UO_2 precusor, which suggested that the volatilization of Cs and UO_2 was not congruent.

3.2. CsI + stoichiometric urania

Cesium iodide was heated along with the freshly crushed, unirradiated fuel, and the annealed fuel, in separate tests. The cesium-ion signal was converted to partial pressure (Pa) and was plotted for these runs as a function of reciprocal temperature, Fig. 3. The results for the unannealed and the annealed urania were very similar, showing that the preparation had little effect on the chemistry of the urania.

The types of ions and their intensities recorded as the CsI – $UO_{2.00}$ mixture was heated up to 1000 K were similar to those observed when heating pure CsI. Above 1000 K, Cs^+, I^+ and CsI^+ were observed, which were not seen when pure CsI was heated in the Knudsen cell. It was possible that the CsI adsorbed onto the UO_2, and then was vaporized between 1000 and 1200 K.

$$\mathrm{CsI(adsorbed\ on\ UO_2)} \Rightarrow \mathrm{CsI(g)}. \quad (3)$$

This phenomenon has also been observed in previous experiments (J. McFarlane and J.C. LeBlanc, unpublished data, 1994) when CsI was heated in contact with a ThO_2 ceramic. The suspicion that surface adsorption was play-

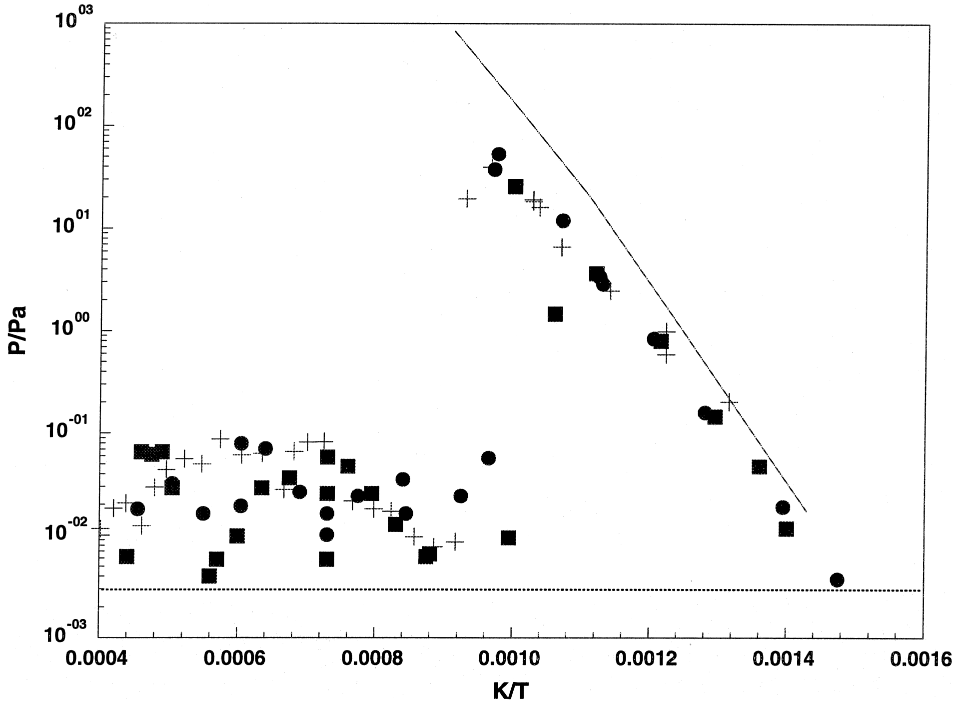

Fig. 3. Partial pressure (Pa) of cesium compounds as a function of reciprocal temperature (K^{-1}) above a mixture of 4 wt% CsI and $UO_{2.00\pm0.01}$. Solid symbols are data from unannealed $UO_{2.00}$ and crosses are from annealed $UO_{2.00}$, respectively. Data represented by squares were collected using a tantalum Knudsen cell and by circles, in an iridium-coated Knudsen cell. The dashed line indicates the detection limit of the experiment. The solid line is published vapour-pressure data for CsI [2].

ing a role was strengthened by the observation that 100 times more signal was observed in this region when the particle size of the dioxide was reduced by a factor of 10 (increasing the surface area by a factor of 10). Trapping of CsI through chemisorption is thought to be less likely, because the volatilized CsI observed at the higher temperatures gave the same ionic signature as the lower temperature CsI.

3.3. CsI + highly oxidized urania

Cesium iodide and highly oxidized urania, $UO_{2.29\pm0.01}$, were heated in combination to increase the yield of the reaction between CsI and UO_{2+x} to allow identification of products by post-test XRD analysis. The results of heating CsI (4–5 wt%) and $UO_{2.29}$ between 1300 and 1700 K in an iridium-coated tantalum cell are displayed in Fig. 4. The partial pressures of the cesium species are shown as a function of reciprocal temperature, with replicate runs indicated by squares and triangles.

Appearance potential measurements on the individual cesium ions were done to show whether fragmentation in the ionizer of the mass spectrometer was of a concern, and to give the identity of the parent molecule (Table 3). The appearance potential of Cs^+ observed between 800 and 1000 K was 7.7 ± 0.2 eV, indicating that the Cs^+ originated from the breakup of the parent CsI [15]. The appearance potential of Cs^+ at 1200 ± 50 K was very similar, 7.4 ± 0.2 eV, suggesting that the Cs^+ came once more from CsI dissociation. The appearance potential of the Cs^+ at 1629 K was 3.8 ± 0.2 eV, suggesting that the parent species was atomic Cs.

An ion signal from molecular iodine was observed at lower temperatures, 650–900 K, which dropped off as the sample was heated above this temperature. The $m/z = 254$ signal was thought to come from I_2^+ directly rather than from the fragmentation of $Cs_2I_2^+$, because the temperature dependence of the signal from $m/z = 254$ was quite different from that of other cesium iodide-derived ions ($m/z = 127$ (I^+), $m/z = 260$ (CsI^+) and $m/z = 393$ (Cs_2I^+)), the latter which parallel the Cs^+. In addition, electron impact ionization studies of cesium iodide do not report the formation of I_2^+ as being significant [16]. The iodine was likely a product of the reaction of CsI in the cell. Although a $m/z = 254$ also corresponds to UO^+, this species would not have been present between 650 and 900 K. Ions from the volatilization of UO_2, including UO^+, were observed at temperatures above 2000 K, Table 1.

Because the thermodynamic and appearance-potential data suggested that the CsI + UO_{2+x} system was reactive, the condensed phase was analyzed by XRD after

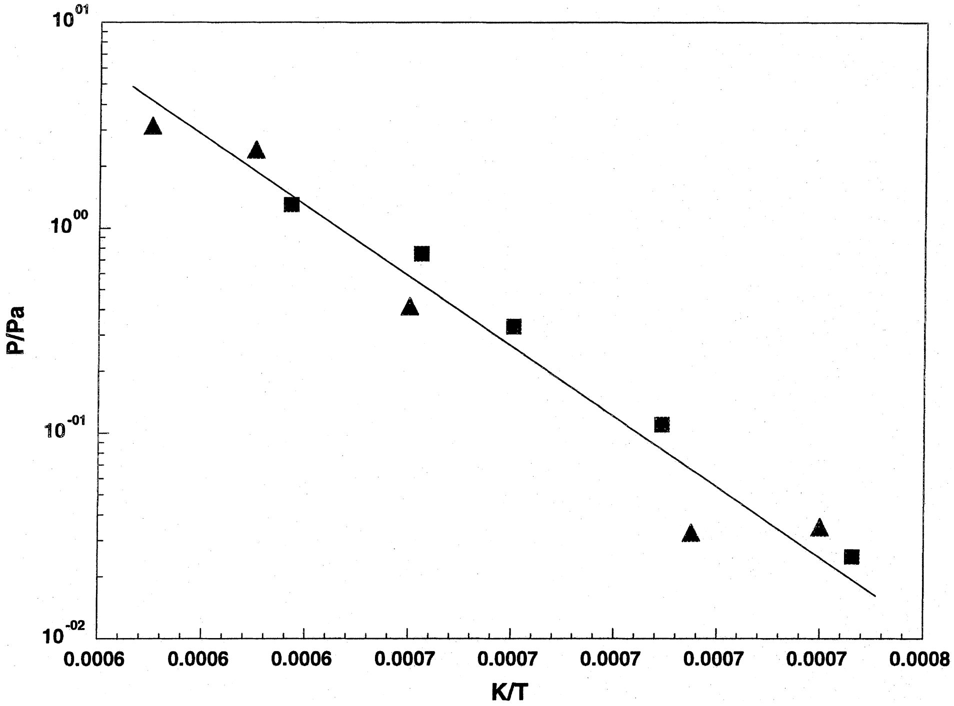

Fig. 4. Partial pressure (Pa) of cesium above CsI – $UO_{2.29}$ as a function of reciprocal temperature (K^{-1}). Replicate runs are indicated by the different symbols. The detection limit of the experiment is 10^{-2} Pa.

being heated. A mixture of 11.4 wt% CsI in $UO_{2.29}$ was heated to 1479 K. By this temperature the iodine signal had disappeared, indicating that the CsI had either volatilized or reacted. Weighing of the sample after the test suggested that 44% of the Cs from the cesium iodide was present after heating. Results of the XRD analysis indicated a substantial amount of $Cs_2U_4O_{12}$ was present. If allowed to cool slowly below 873 K the $Cs_2U_4O_{12}$ will disproportionate into a number of mixed phases, such as $Cs_2U_5O_{16}$ + $Cs_2U_4O_{13}$ [17]; however, these were not observed in the XRD analysis. Continued heating of the same sample to 1800 K depleted most of the cesium signal seen by the mass spectrometer. X-ray diffraction analysis of this sample showed that most of the cesium uranate had disappeared, leaving only a trace in with the UO_2.

3.4. High-temperature reactions of CsI and urania

Measured heats of vaporization, ion appearance potentials and XRD analysis allowed the species volatilized from the mixture of CsI and $UO_{2.29}$ to be identified. At the lowest temperatures, between 650 and 1000 K, the volatilization of CsI occurred, and Cs^+, I^+, CsI^+ and Cs_2I^+ were observed in the mass spectrometer.

$$\mathrm{CsI(s)} \Rightarrow \mathrm{CsI(g), Cs_2I_2(g)}. \tag{4}$$

A heat of vaporization to CsI(g) was measured, $\Delta_v H^0$ (298.15 K) = 202 ± 5 kJ mol^{-1}. As in the case of pure CsI discussed earlier, the result was higher than that given in the literature for pure CsI [2].

Residue remaining in the cell after heating to 1479 K was identified by XRD analysis as $Cs_2U_4O_{12}$, a reaction product of CsI and $UO_{2.29}$, Reaction (5), as previously suggested by Ugajin [18]:

$$\begin{aligned} &\mathrm{2CsI(s)} + \left(\frac{4}{x}\right)\mathrm{UO_{2+x}(s)} \\ &\Rightarrow \mathrm{Cs_2U_4O_{12}(s)} + \mathrm{I_2(g)} + \left(\frac{4}{x}\right)(1-x)\mathrm{UO_2(s)}. \end{aligned} \tag{5}$$

As it is heated in a vacuum, cesium uranate decomposes, releasing Cs and oxygen, Reaction (6) [17]. (No cesium oxide was observed in the mass spectrometer.)

$$\mathrm{Cs_2U_4O_{12}(s)} \Rightarrow \mathrm{4UO_2(s)} + \mathrm{2Cs(g)} + \mathrm{2O_2(g)}. \tag{6}$$

That the cesium signal between 1250 and 1700 K arises from a uranate phase is consistent with the fact that the $UO_{2.29}$ produced 100 times more signal in this temperature range than did $UO_{2.00}$. This is because formation of $Cs_2U_4O_{12}$ (or any other uranate) requires uranium to be oxidized beyond the +4 state. In addition, no iodine was observed in this region, confirming that the cesium did not come from CsI revolatilization. Scatter in the partial-pressure data between 1600 and 1700 K may be attributed to interconversion of cesium uranate phases, such as

$$3Cs_2U_4O_{12}(s) = 2Cs_2U_6O_{18}(s) + 2Cs(g). \quad (7)$$

The condensed phase becomes depleted in cesium during the process. The post-test XRD analysis was not sensitive enough to confirm such a shift in composition, being limited to about 4 wt%.

Because it is a logarithmic plot, Fig. 4 gives a distorted picture of the relative amounts of Cs^+ species volatilized as a function of temperature. Consequently the vapour pressure of Cs^+ ion has been plotted versus time over the experimental run, on a linear scale, as shown in Fig. 5. The quantity of Cs^+ in each peak becomes apparent: about 50% of the CsI starting material was volatilized as CsI below 1000 K, and the rest was converted to cesium uranate and subsequently released between 1250 and 1800 K. A small amount, less than 1%, was released between 1000 and 1250 K, and only 0.1% remained above 1800 K.

3.5. Control of oxygen potential by urania

When the decomposition of $Cs_2U_4O_{12}$ to UO_2 is studied, Reaction (6), it is apparent that at a given temperature at equilibrium, the pressure of the cesium and the oxygen in the system are not independent, as shown in Eq. (8):

$$\Delta_r G^0(T) = -2RT \ln P_{Cs}P_{O_2}. \quad (8)$$

The question to be addressed is what is giving rise to the partial pressures observed in the Knudsen cell. Are they strictly based on Reaction (6) alone, or is there external control of partial pressure of oxygen in the system? Unfortunately, the partial pressure of the oxygen could not be measured directly in the Knudsen cell, because of the background, so it was determined from the measured partial pressure of cesium and Eq. (8). The partial pressure of cesium was much higher than the partial pressure of oxygen in this experiment. Auxiliary data, the Gibbs free energies as a function of temperature for the species in Reaction (6), came from Cordfunke and Konings [2].

The derived oxygen potential, defined here as $RT\ln PO_2$, is plotted in Fig. 6 as a function of reciprocal temperature. If the decomposition of $Cs_2U_4O_{12}$ governed the oxygen partial pressure in the Knudsen cell between 1250 and 1700 K, Reaction (6), the partial pressures of cesium and oxygen would be the same [17]. This was not the case for the system under investigation. Likewise, the pressure of oxygen was not set by the baseline amount of oxygen in the Knudsen cell ($<10^{-5}$ Pa), or by the formation of $Ta_2O_5(\beta)$ in the tantalum cell ($<5 \times 10^{-5}$ Pa) [19].

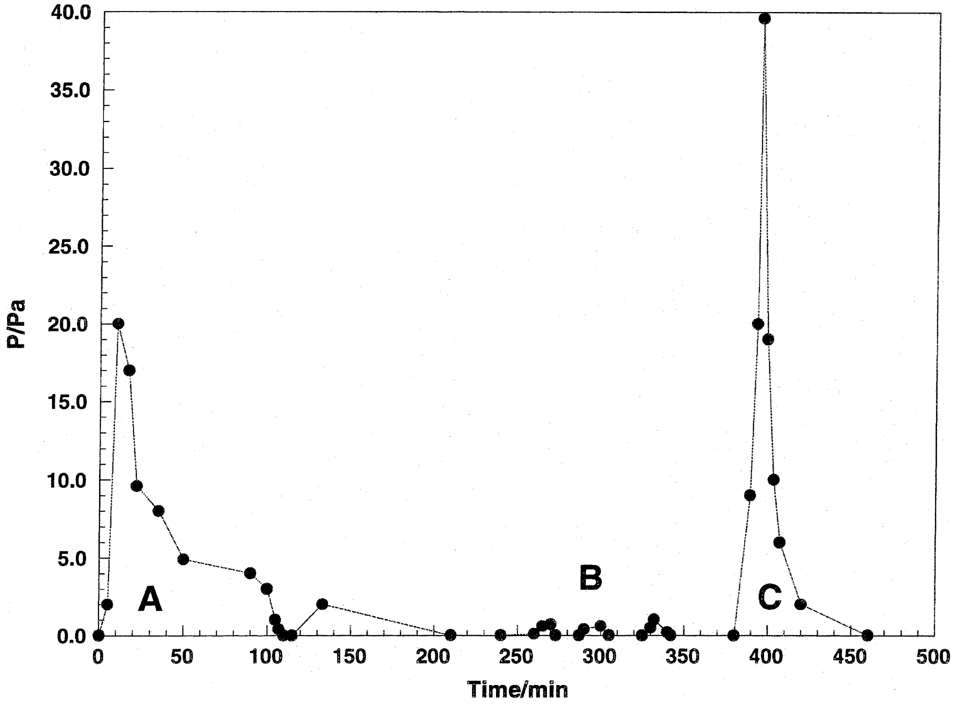

Fig. 5. Plot of partial pressure (Pa) of cesium species as a function of time (min). Cesium species are evolved from a mixture of CsI + $UO_{2.29}$, during descending ramps in temperature. Double-humped peak A shows data that were collected between 1000 and 800 K. The scatter of points, B, refers to data that were collected between 1230 and 1570 K. The sharp peak, C, was collected at 1770 ± 5 K.

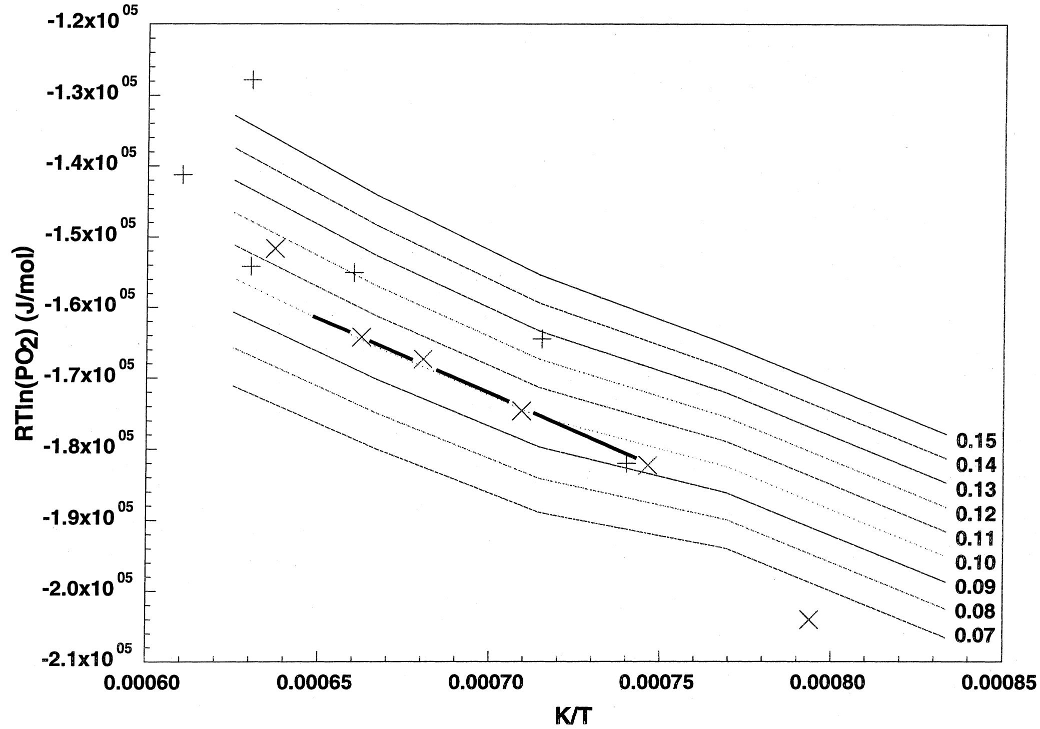

Fig. 6. Oxygen chemical potential (J mol^{-1}) as a function of $1/T$ (K^{-1}). Calculated values of oxygen potential in equilibrium with UO_{2+x} represented as a solid solution of UO_2/U_3O_7 are shown as lines on the plot, annotated by the value of x in UO_{2+x}. The data for two separate tests are shown as symbols.

Another possibility was control of the oxygen by the urania in the cell, by having an equilibrium established between UO_{2+x} and O_2. The partial pressure of oxygen above UO_{2+x} has been characterized by an empirical formulation [20]. Using the criteria set out by Lindemer and Besmann, in the current experiment the UO_{2+x} could be represented as a solid solution of UO_2/U_3O_7. Calculated oxygen potentials over UO_{2+x} from $0.07 < x < 0.15$ are plotted in Fig. 6 as solid lines. Superimposed with the lines are points derived from two separate experiments involving CsI and $UO_{2.29}$. As can be seen from the graph, for one of the tests (marked by x), the oxygen potential appeared to be controlled by $UO_{2.10\pm0.01}$ from 1350 to 1580 K, as indicated by the bold line drawn through the data points. Data for another run (marked by +) were not as conclusive; however, it can be reported that in this case the urania in equilibrium with the uranate was $UO_{2.11\pm0.02}$ from 1350 to 1590 K.

3.6. Comparison to related work

The reactivity of the CsI – UO_{2+x} system has been investigated by Ugajin et al. [18]. These authors conducted the experiments at 1073 K, and carefully varied the oxygen potential by manipulating the CO/CO_2 atmosphere to which the sample was exposed. The samples were then analyzed by XRD, and the analytical results were compared to thermochemical calculations.

At 1073 K, the system of CsI – $UO_{2.051}$ was found to be reactive, forming $Cs_2U_4O_{12}$. According to calculation, the poly-uranate will be stable at oxygen potentials between −209 and −260 kJ mol^{-1} at this temperature. At lower oxygen potentials, Cs_2UO_4 is the predominate cesium uranate species. Our study of the CsI – UO_{2+x} system as a function of temperature is in agreement with these data, showing that the system can react to form cesium uranate, $Cs_2U_4O_{12}$ from CsI – $UO_{2.29}$. As temperatures were increased above 1300 K, in a vacuum, the cesium uranate decomposed to UO_2.

Ugajin and co-workers [18] also predicted the equilibrium iodine pressure, I and I_2, above the CsI – UO_{2+x} mixture as a function of temperature. They determined the pressure as being little different from the pressure above pure CsI. These pressures are very low, being of the order of 0.01 Pa at 1060 K. It was not possible to measure the iodine partial pressure in the current Knudsen-cell experiment, because it was not in chemical equilibrium with the condensed phase. Reproducible results could not be achieved between ascending and descending temperature ramps, unlike in the case of the higher temperature CsI and Cs results. The iodine was liberated by the decomposition of CsI, and was slowly depleted from the Knudsen cell as the experiment continued.

4. Conclusions

The final data obtained for 4 wt% CsI in $UO_{2.00}$ and $UO_{2.29}$ could not have been obtained without first eliminating all the artifacts. Differences in the various temperature regions of the CsI/UO_{2+x} reaction would have easily been swamped by signal either from revolatilization or reactions with cell materials (such as tungsten). Cesium iodide was shown to react with the excess oxygen in urania, producing $Cs_2U_4O_{12}$. The reactivity of the system and the decomposition of the uranate above 1250 K appeared to be governed by the chemical potential of oxygen of the urania in the sample. This phenomenon may also govern the speciation of cesium and iodine found in irradiated UO_2 reactor fuel.

Acknowledgements

The authors would like to thank Dr P. Taylor for his assistance both during the experiments, in particular with the analysis of the XRD data, and in reviewing the document. Other helpful criticism has come from Drs R.J. Lemire and R. McEachern.

References

[1] D. Wren, Kinetics of Iodine and Cesium Reactions in the CANDU Reactor Primary Heat Transport System under Reactor Accident Conditions, Atomic Energy of Canada Limited Report, AECL-7781, 1983.
[2] E.H.P. Cordfunke, R.J.M. Konings (Eds.), Thermochemical Data for Reactor Materials and Fission Products, North-Holland, Amsterdam, 1990, pp. 110–119; 158–160.
[3] Hj. Matzke, J. Nucl. Mater. 208 (1994) 18.
[4] D.S. Cox, F.C. Iglesias, C.E.L. Hunt, N.A. Keller, R.D. Barrand, R.F. O'Connor, J.R. Mitchell, in: Proc. of the Eighth Annual Conf. of the Canadian Nuclear Society, June 16–17, St. John, NB, Canada, 1987, pp. 58–63.
[5] R.P. Iczkowski, J.L. Margrave, S.M. Robinson, J. Phys. Chem. 67 (1963) 229.
[6] J. McFarlane, J.C. LeBlanc, D.G. Owen, Proc. of the Fourth Int. Conf. on CANDU Fuel, Pembroke, Ont., Canada, October 1–4, Canadian Nuclear Society, 1995, pp. 6B-1-6B-10.
[7] Binary Alloy Phase Diagrams, ASM International Handbook, vol. 3, The Materials Information Society, Materials Park, OH, 1992.
[8] J.C. Tait, I.C. Gauld, G.B. Wilkin, Derivation of Initial Radionuclide Inventories for the Safety Assessment of the Disposal of Used CANDU® Fuel, Atomic Energy of Canada Limited Report, AECL-9881, 1989.
[9] E. Storms, High Temp. Sci. 1 (1969) 456.
[10] J.C. LeBlanc, J. McFarlane, High Temp. High Press. 26 (1994) 401.
[11] E.J. McGuire, Phys. Rev. A 20 (1979) 445; J. Kordis, K.A. Gingerich, J. Chem. Phys. 68 (1973) 5141; J.B. Mann, in: R. Ogata, T. Hanakawa (Eds.), Recent Developments in Mass Spectroscopy, University Press, Tokyo, 1970, p. 814; J.W. Otvos, D.P. Stevenson, J. Am. Chem. Soc. 78 (1955) 546; P.E. Blackburn, P.M. Danielson, J. Chem. Phys. 56 (1972) 6156; J.C. Halle, H.H. Lo, W.L. Fite, Phys. Rev. A 23 (1981) 1708.
[12] M.W. Chase Jr., C.A. Davies, J.R. Downey Jr., D.J. Frurip, R.A. McDonald, A.N. Syverud, JANAF Thermochemical Tables, 3rd ed., Part 1, Al-Co, J. Phys. Chem. Ref. Data 14, Supplement No. 1, 1985, pp. 14–15.
[13] J. McFarlane, J.C. LeBlanc, Alkali-Iodide Systems at High Temperatures I. Cesium Uranate Chemistry, Atomic Energy of Canada Limited Report, AECL-11118, 1994.
[14] H. Kleykamp, J. Nucl. Mater. 131 (1985) 221.
[15] J.L. Franklin, J.G. Dillard, Ionization Potentials, Appearance Potentials, and Heats of Formation of Gaseous Positive Ions, Nat. Stand. Ref. Data Ser., Nat. Bur. Stand., US, NSRDS-NBS 26, pp. 223–224; 228–229.
[16] R. Viswanathan, K. Hilpert, Ber. Bunsenges. Phys. Chem. 88 (1984) 125.
[17] E.H.P. Cordfunke, Thermodynamics of Nuclear Materials, Proceedings of an IAEA Symposium, Vienna, October 21–25, IAEA-SM-190/6, 1974, pp. 185–192.
[18] M. Ugajin, T. Nagasaki, A. Itoh, J. Nucl. Mater. 230 (1996) 195.
[19] L.B. Pankratz, Thermodynamic Properties of Elements and Oxides, Bulletin, US Bureau of Mines, 672 (1982).
[20] T.B. Lindemer, T.M. Besmann, J. Nucl. Mater. 130 (1985) 473.